



Anomalous hybridization in the In-rich InAs(0 0 1) reconstruction

Darby L. Feldwinn^{a,1}, Jonathon B. Clemens^a, Jian Shen^a, Sarah R. Bishop^a, Tyler J. Grassman^{a,2}, Andrew C. Kummel^{a,*}, Ravi Droopad^{b,3}, Matthias Passlack^{b,4}

^a Department of Chemistry and Biochemistry, University of California, San Diego, 9500 Gilman Dr. #0358, La Jolla, California 92093-0358, USA

^b Freescale Semiconductor, 2100 E. Elliot Road, Tempe, Arizona 85283, USA

ARTICLE INFO

Article history:

Received 23 July 2009

Accepted for publication 23 September 2009

Available online 29 September 2009

Keywords:

Density functional calculations
Scanning tunneling microscopy
Indium arsenide
Semiconducting surfaces
Surface relaxation and reconstruction

ABSTRACT

The surface bonding arrangement in nearly all the confirmed reconstructions of InAs(0 0 1) and GaAs(0 0 1) have only two types of hybridization present. Either the bonds are similar to those in the bulk and the surface atoms are sp^3 hybridized or the surface atoms are in a tricoordinated bonding arrangement and are sp^2 hybridized. However, dicoordinated In atoms with sp hybridization are observed on the InAs(0 0 1), In-rich, room temperature and low temperature surfaces. Scanning tunneling microscopy (STM) images of the room temperature (300 K) InAs(0 0 1) surface reveal that the In-rich surface reconstruction consists of single-atom rows with areas of high electron density that are separated by ~ 4.3 Å. The separation in electron density is consistent with rows of undimerized, sp hybridized, In atoms, denoted as the $\beta 3'(4 \times 2)$ reconstruction. As the sample is cooled to 77 K, the reconstruction spontaneously changes. STM images of the low temperature surface reveal that the areas of high electron density are no longer separated by ~ 4.3 Å but instead by ~ 17 Å. In addition, the LEED pattern changes from a (4×2) pattern to a (4×4) pattern at 77 K. The 77 K reconstruction is consistent with two (4×2) subunit cells; one that contains In dimers on the row and another subunit cell that contains undimerized, sp hybridized, In atoms on the row. This combination of dimerized and undimerized subunit cells results in a new unit cell with (4×4) periodicity, denoted as the $\beta 3(4 \times 4)$ reconstruction. Density functional theory (DFT) and STM simulations were used to confirm the experimental findings.

© 2009 Elsevier B.V. All rights reserved.

1. Introduction

Due to its high electron mobility ($30,000 \text{ cm}^2 \text{ V}^{-1} \text{ s}^{-1}$), InAs is a potential channel material for III–V metal-oxide-semiconductor field effect transistors (MOSFETs) [1]. Formation of a defect-free oxide–InAs interface is a key challenge in InAs MOSFET development. During the growth of the gate oxide layer using techniques such as molecular beam epitaxy (MBE) or atomic layer deposition (ALD), the InAs surface may be exposed to oxygen [2,3]. Since oxygen has been shown to cause defects and Fermi level pinning on

other III–V surfaces [4–6] it would be preferable to find an InAs surface that is relatively unreactive to oxygen. The InAs(0 0 1)– (4×2) surface has been shown to have very low reactivity to molecular oxygen [7] making it a viable potential starting template for subsequent ALD or MBE growth in MOSFET fabrication. However, the In-rich InAs(0 0 1) surface reconstruction is not well understood, and having an atomic understanding of the clean surface is critical. A clear understanding of the surface structure allows for the analysis of defects, expands the knowledge base of semiconductor surfaces, and aids in the development of new and specific chemistry.

Since InAs and GaAs have similar chemical properties, it might be assumed that the (4×2) reconstruction of the two semiconductors would be the same. However, scanning tunneling microscopy (STM) images of the two surfaces differ dramatically. Despite the differences in STM images between InAs(0 0 1)– (4×2) and GaAs(0 0 1)– (4×2) reconstructions [4,6,8–11], some computational studies still propose that the InAs structure is the $\zeta(4 \times 2)$ [11,12] reconstruction that has been well documented for GaAs. Both of the theoretical studies that conclude the InAs (4×2) structure was the $\zeta(4 \times 2)$ reconstruction did not employ STM for comparison to the structural model, and one study did not compare the $\beta 3$ model to other structures they proposed. Other studies have

* Corresponding author. Tel.: +1 858 534 3368; fax: +1 858 534 2063.

E-mail addresses: feldwinn@chem.ucsb.edu (D.L. Feldwinn), jclemens@ucsd.edu (J.B. Clemens), jimshen@ucsd.edu (J. Shen), sbishop@ucsd.edu (S.R. Bishop), grassman@ece.osu.edu (T.J. Grassman), akummel@ucsd.edu (A.C. Kummel), rdroopad@txstate.edu (R. Droopad), matthias_passlack@tsmc.com (M. Passlack).

¹ Present address: Chemistry Department, University of California, Santa Barbara, Santa Barbara, CA 93106-9560, USA.

² Present address: Department of Electrical and Computer Engineering, The Ohio State University, 205 Dreese Laboratory, 2015 Neil Ave., Columbus, OH 43210, USA.

³ Present address: Department of Physics, Texas State University–San Marcos, San Marcos, Texas 78666, USA.

⁴ Present address: Taiwan Semiconductor Manufacturing Company Ltd., IMEC vzw, Kapeldreef 75, B-3001 Leuven, Belgium.

proposed different (4×2) structures that include the $\alpha(4 \times 2)$ [8,9], $\beta_2(4 \times 2)$ [12], and $\beta_3(4 \times 2)$ [4,10,13]. These structures along with four other possible (4×2) reconstructions [$\alpha_2(4 \times 2)$, $\alpha_3(4 \times 2)$, $\beta(4 \times 2)$, and $S(4 \times 2)$] are shown in Fig. 1. Although numerous studies have attempted to determine the InAs(001)- (4×2) reconstruction, the majority focused either on experimental determination [4,8,13] or computational determination [11,12,14] of the surface but did not employ both techniques. In addition, many of the computational studies only considered a

small subset of the possible (4×2) reconstructions and none of the experimental procedures involved cryogenic experiments.

Experimental and computational studies were employed to determine the room temperature (300 K) and low temperature (77 K) reconstructions of the In-rich InAs(001) surface. Detailed room and low temperature STM images of the clean surface revealed that neither reconstruction was an identical match to the possible (4×2) structures shown in Fig. 1. The 300 K STM images identified that the most probable InAs(001)- (4×2) reconstruction was similar to the $\beta_3(4 \times 2)$ structure. However, instead of having row In atoms that were dimerized, the row In atoms were undimerized, thereby making it the $\beta_3'(4 \times 2)$ structure. The $\beta_3'(4 \times 2)$ structure consists of rows of sp hybridized, dicoordinated In atoms which run in the $[1\ 1\ 0]$ direction. As the sample was cooled from room temperature to 77 K, low energy electron diffraction (LEED) revealed that the sample underwent a spontaneous and reversible change in surface periodicity from a (4×2) reconstruction to a (4×4) reconstruction. STM images confirmed that the real space periodicity of areas of high electron density changed from ~ 4.3 Å to ~ 17 Å. LEED and STM findings suggested that the 77 K surface reconstruction results from the combination of two (4×2) unit cells; one subunit cell being a $\beta_3(4 \times 2)$ unit cell and the other subunit cell being a $\beta_3'(4 \times 2)$ unit cell. This results in a new unit cell with (4×4) periodicity denoted as the $\beta_3(4 \times 4)$ reconstruction. Density functional theory (DFT) calculations were performed to confirm the experimental findings.

2. Experimental and computational techniques

Experiments were performed in two different UHV chambers that were both equipped with a LEED and an STM. One chamber housed a Park Scientific VP STM while the other chamber housed an Omicron LT STM. Images taken with the Omicron STM are labeled within the text of the paper. In addition, the Omicron machine was capable of taking STM images at both 300 K and 77 K. As₂-capped InAs(001) samples were grown offsite via MBE on epi-ready wafers and then were transferred into one of the UHV chambers. The samples were then thermally decapped to produce the In-rich InAs(001) surface by different procedures in the two STM chambers. In the Park Scientific VP STM chamber, the wafers were decapped by performing ramping cycles to ~ 450 °C as previously described.[15] In the Omicron LT STM chamber, the wafers were decapped by radiantly heating the sample via a PBN sample stage heater as described previously.[7] In both chambers, after the decapping procedure was complete, LEED was used to verify the surface periodicity, after which the samples were transferred into the STM for analysis. Both LEED and STM data from each chamber show that both preparation methods produce the identical $\beta_3'(4 \times 2)$ reconstruction of the InAs(001) surface at room temperature. Atomically resolved STM images were recorded at both 300 K and 77 K with the Omicron machine.

Other STM studies of decapped InAs(001) have been performed and revealed similar room temperature (4×2) STM images. In addition, no other (4×2) reconstructions have been seen by this group or published by other groups for thermally decapped samples. The authors concede that other (4×2) reconstructions may be possible on non As-capped MBE grown samples; however, there are no published STM studies on in situ grown (4×2) reconstructions. Therefore, the focus of this paper will be on the reconstructions that correlate to current and previous STM studies on decapped samples.

DFT calculations were used to confirm and interpret the experimental results. Plane wave (periodic boundary) calculations were performed using the Vienna *ab-initio* simulation package (VASP) code on double slabs (two (4×2) unit cells) [16–19]. The current

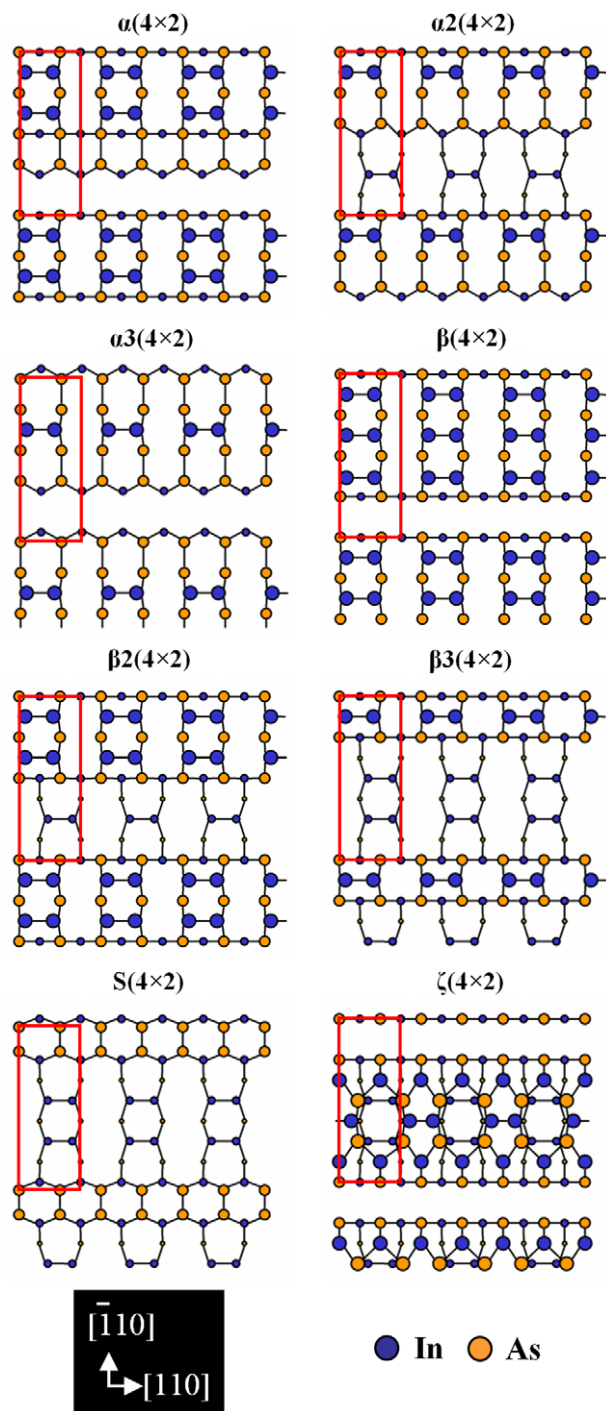


Fig. 1. Ball-and-stick diagrams of the possible structures for the InAs(001)- (4×2) reconstruction. The red boxes denote the unit cells of each reconstruction. (For interpretation of the references to colour in this figure legend, the reader is referred to the web version of this article.)

study employed a nine-atomic-layer slab which has pseudo-hydrogen atoms with a charge of $1.25 e^-$ terminating the bottom layer. In order to preserve the bulk-like properties of the system, the bottom three layers of the slab, along with the pseudo-hydrogen atoms, were frozen in the bulk position. In addition, thirteen layers of vacuum were used to minimize interactions between the top and bottom of the slabs. Calculations were performed using the Perdew–Burke–Ernzerhof (PBE) [20] variant of the general gradient approximation. Atoms were modeled using projector augmented wave (PAW) [21,22] potentials as supplied by VASP. A $2 \times 4 \times 1$ Monkhorst–Pack k -point sampling scheme was employed which resulted in the generation of 4 irreducible k -points in the first Brillouin zone. The plane wave cut off energy was set to 500 eV. The relaxation criteria were set to terminate the calculations once the forces were below 0.05 eV/Å.

3. Experimental results and discussion

3.1. 300 K In-rich InAs(0 0 1) reconstruction

A large scale ($450 \text{ \AA} \times 450 \text{ \AA}$) 300 K STM image of the clean In-rich (4×2) reconstruction is shown in Fig. 2a. The image shows bright, long straight rows that run in the $[1 \ 1 \ 0]$ direction. The rows are separated by $\sim 17 \text{ \AA}$ and have a thickness of $\sim 7 \text{ \AA}$. The effects of sample bias on the STM images were also explored. The bias-dependent images showed that the trough structure is more readily resolved in empty state images than in filled state images, as was noted by other groups [4,13]. The STM results allow for the elimination of many of the proposed real space (4×2) structures (Fig. 1).

Although InAs and GaAs have similar chemical properties and both have group-III rich (4×2) reconstructions on the (0 0 1) surface, the real space $\zeta(4 \times 2)$ structure for the GaAs(0 0 1)-(4×2) [11,14,23,24] surface is inconsistent with the InAs(0 0 1)-(4×2) STM images. Comparing the STM images from GaAs and InAs studies reveal that the GaAs(0 0 1)-(4×2) reconstruction has thicker rows than the (4×2) reconstruction on InAs(0 0 1). Furthermore, the periodicity of the trough structure on the $\zeta(4 \times 2)$ reconstruction in the $[1 \ 1 \ 0]$ direction is only $\sim 4.3 \text{ \AA}$ instead of the $\sim 8.5 \text{ \AA}$ observed in the STM data from this study. Therefore the $\zeta(4 \times 2)$ structure can be eliminated as a possible reconstruction for the InAs(0 0 1)-(4×2) surface.

One of the physical attributes of InAs(0 0 1)-(4×2) STM images are straight rows which do not zigzag. This implies that the reconstruction cannot have multiple, nearly degenerate structures. An example of a structure with two nearly degenerate reconstructions is the $\alpha 2(4 \times 2)$ reconstruction. For the $\alpha 2(4 \times 2)$ reconstruction as shown in Fig. 1, the In dimer can either occur on the top portion of the row or the bottom portion of the row. Since the structures are energetically degenerate, the experimental surface would contain a distribution of the sites, causing the rows to appear to zigzag in STM images [25]. Since all of the reconstructions in the “ α ” series [$\alpha(4 \times 2)$, $\alpha 2(4 \times 2)$, and $\alpha 3(4 \times 2)$] contain nearly degenerate reconstructions, all of the α reconstructions can be eliminated as possible real InAs(0 0 1)-(4×2) structures.

Atomically resolved STM images of the trough region (Fig. 2b) on the In-rich InAs(0 0 1) reconstruction reveal the experimental periodicity in the bright trough regions is $\sim 8.5 \text{ \AA}$. In addition, the STM image clearly shows double dimers in the trough region. The information gleaned from the trough structure allows for the elimination of two other structures, the $\beta(4 \times 2)$ and the $\beta 2(4 \times 2)$ reconstructions. The $\beta(4 \times 2)$ reconstruction would be expected to have trough spacing of $\sim 4.3 \text{ \AA}$ instead of the $\sim 8.5 \text{ \AA}$ experimentally observed; in addition the $\beta(4 \times 2)$ structure has no dimers in the trough region. Whereas, the $\beta 2(4 \times 2)$ reconstruc-

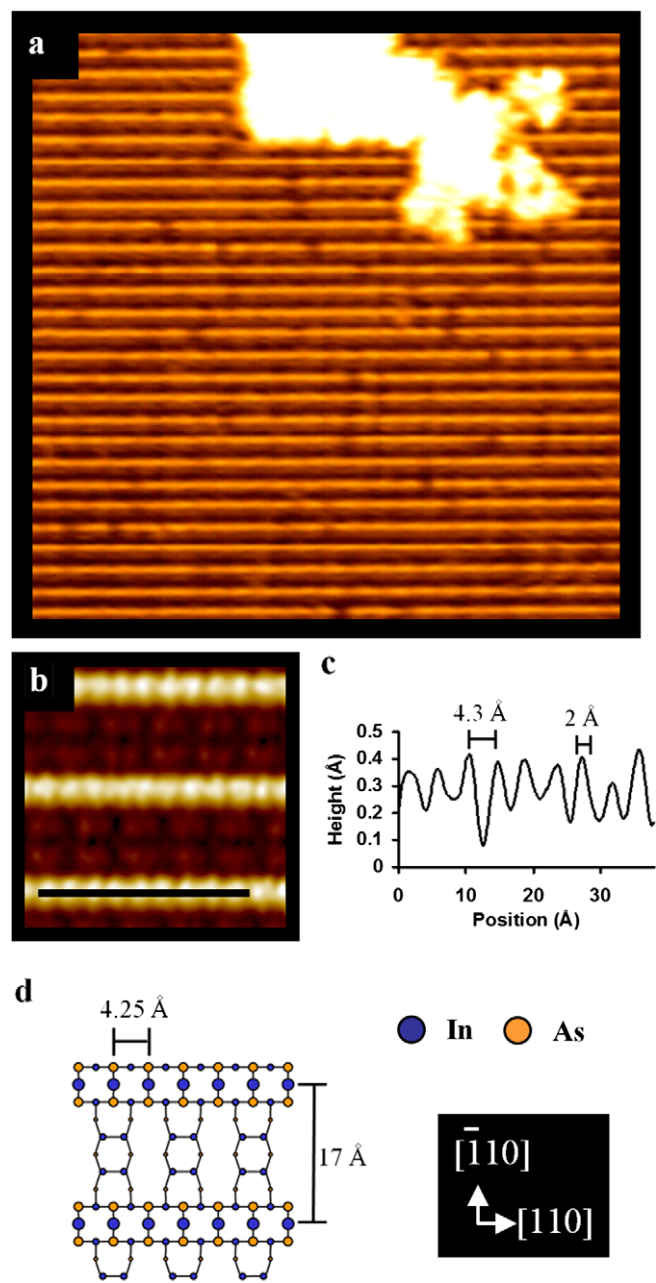


Fig. 2. (a) $450 \text{ \AA} \times 450 \text{ \AA}$ large scale STM image ($V_s = -2 \text{ V}$, $I_t = 0.5 \text{ nA}$) of the InAs(0 0 1)-(4×2) surface. (b) $50 \text{ \AA} \times 50 \text{ \AA}$ atomically resolved STM image ($V_s = -1.5 \text{ V}$, $I_t = 0.05 \text{ nA}$). (c) Line scan corresponding to the black line on the STM image revealing that areas of increased electron density are separated by $\sim 4.3 \text{ \AA}$. (d) Ball-and-stick diagram of the $\beta 3'(4 \times 2)$ reconstruction.

tion has only 1 dimer in the trough as opposed to the double dimers that are seen experimentally.

The remaining two structures, the $\beta 3(4 \times 2)$ and $S(4 \times 2)$, can be distinguished from each other by examining row thicknesses. The experimentally observed rows on InAs(0 0 1)-(4×2) are only $\sim 7 \text{ \AA}$ wide. The GaAs(0 0 1)-(2×4) surface is very well documented to have double As dimer rows, which image $\sim 9 \text{ \AA}$ wide in STM [26]. Since the InAs rows are thinner than the GaAs(0 0 1)-(2×4) rows, this suggests that the (4×2) structure has rows which are a single dimer wide. This is further supported by a comparison of the InAs and GaAs lattice constants. The lattice constant of InAs is larger than the lattice constant of GaAs by about 0.4 \AA [27]. If the InAs(0 0 1)-(4×2) reconstruction had the identi-

cal double dimer row configuration of the GaAs(001)-(2 × 4) reconstruction, the bright row would appear even thicker in STM images for InAs, which was not found experimentally. Although the S(4 × 2) reconstruction only has a single dimer row, the row As dimers are aligned in the $[\bar{1}10]$ direction; therefore, the As filled dangling bonds point into the trough. This would cause the rows on the S(4 × 2) reconstruction to appear wider than a structure that contained double dimers which run in the $[1\bar{1}0]$ direction. Therefore, the most probable structure from Fig. 1 is the $\beta_3(4 \times 2)$ reconstruction.

Atomically resolved STM images indicate that the InAs(001)-(4 × 2) reconstruction deviates slightly from the expected fully dimerized $\beta_3(4 \times 2)$ reconstruction. Figs. 2b and c show an atomically resolved STM image along with a line scan down the length of one of the InAs(001)-(4 × 2) rows scanned by the Omicron system. The line scan reveals that regions of high electron density are periodic and occur every ~ 4.3 Å. However, for the fully dimerized $\beta_3(4 \times 2)$ reconstruction one would expect areas of high electron density to occur every ~ 8.5 Å. Therefore, the experimental data suggests that instead of the rows consisting of In dimers, they are comprised of undimerized In atoms. Fig. 2d shows a ball-and-stick diagram of the undimerized $\beta_3(4 \times 2)$ structure (denoted as the $\beta_3'(4 \times 2)$ reconstruction).

The bonding environment of the row In atoms on the $\beta_3(4 \times 2)$ and $\beta_3'(4 \times 2)$ surfaces are drastically different. On the $\beta_3(4 \times 2)$ surface each In atom is bonded to one other row In atom and two second layer As atoms. This results in sp^2 hybridized row In atoms. III–V semiconductor surfaces typically only have surface atoms which are either sp^2 or sp^3 hybridized. However, if the In atoms are undimerized, as in the case of the $\beta_3'(4 \times 2)$ reconstruction, the row In atoms form bonds to two second layer As atoms, causing the row In atoms to be sp hybridized. In an sp hybridized system, the As–In–As bond angle should ideally be 180° . Therefore, examining bond angles of the DFT simulated $\beta_3'(4 \times 2)$ surface can further confirm the hybridization of the reconstructed surface atoms.

Similar to the GaAs(001)-c(2 × 8)/(2 × 4) reconstruction [28,29], the location of the trough dimer/dimers in neighboring rows results in two different reconstructions being present on the InAs(001) surface. If the trough dimers are aligned in neighboring rows, the structure is called the InAs(001)-(4 × 2) reconstruction. However, if the trough dimers are shifted by half of a unit cell distance in the $[1\bar{1}0]$ direction, the result is trough dimers in neighboring rows that do not align. This gives rise to a reconstruction that is referred to as the InAs(001)-c(8 × 2) structure. Since both structures will have the same bonding environments and electronic properties, only the (4 × 2) structure will be discussed from here on out.

3.2. 300K In-rich InAs(001) reconstruction

As the InAs(001)-(4 × 2) surface is cooled from 300 K to 77 K, a spontaneous and reversible surface reconstruction change is observed. LEED images taken at 300 K and 77 K are shown in Fig. 3. In the 300 K LEED image (Fig. 3a), each row of diffraction spots is separated by one less well-resolved diffraction streak. In the 77 K LEED image (Fig. 3b), the rows of diffraction spots are separated by three diffraction streaks. This is consistent with the surface reconstruction changing from a (4 × 2) reconstruction to a (4 × 4) reconstruction.

The STM images also change as the InAs(001)-(4 × 2) surface is cooled to 77 K. Fig. 4a shows a $450 \text{ \AA} \times 450 \text{ \AA}$ image of the surface at 77 K obtained on the Omicron system. The 300 K and 77 K images have many similarities such as identical trough structures, single atom-width rows, and no degenerate structures. However, there are two major differences between the row structures that

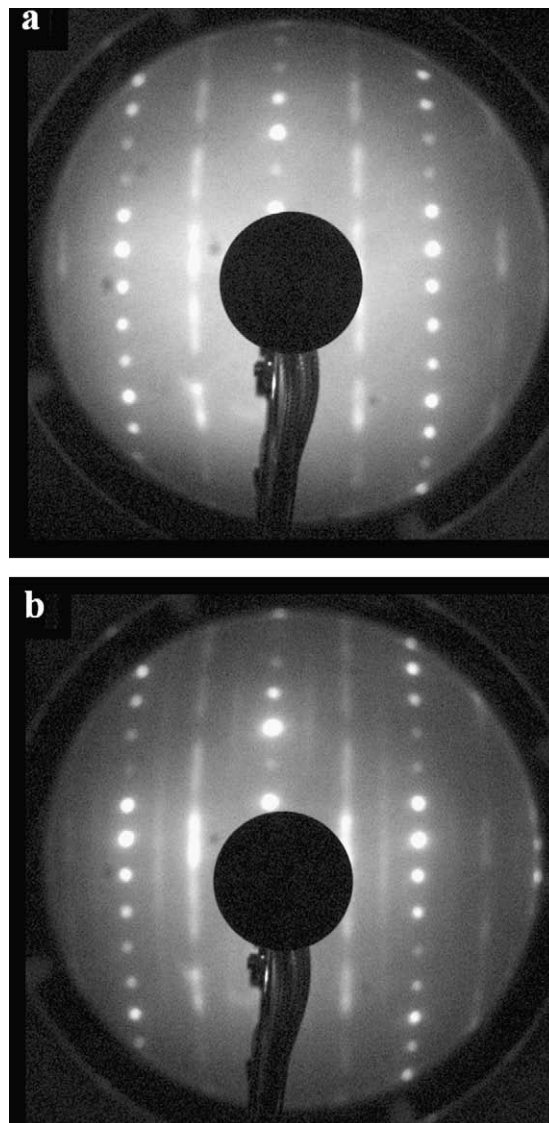


Fig. 3. LEED images of the In-rich InAs(001) surface (a) at 300 K and (b) at 77 K. Showing a change in surface periodicity from a (4 × 2) reconstruction at 300 K to a (4 × 4) reconstruction at 77 K.

can be seen from the atomically resolved STM image, Fig. 4b. First, the line scan (Fig. 4c) of the atomically resolved STM image reveals that the full width at half-maximum of the areas of high electron density along the $[1\bar{1}0]$ direction change from ~ 2 Å at 300 K, to ~ 8 – 10 Å. This is consistent with the row structure changing from single In atoms at 300 K to an In dimer at 77 K. Second, the periodicity of the areas of high electron density along the $[1\bar{1}0]$ direction also changes from ~ 4.3 Å at 300 K to ~ 17 Å at 77 K, as shown in Figs. 2c and 4c respectively. The spacing between the areas of high electron density is consistent with a structural change from a (4 × 2) reconstruction to a (4 × 4) reconstruction.

At 77 K, it is possible that physisorption of ambient gas in the UHV system (such as H₂O, CO₂ and hydrocarbons) occurs on the semiconductor surface. However, this is not believed to result in the change of surface reconstruction for several reasons. First, physisorption does not tend to be site-specific, as would be required for a physisorbate-induced ordered reconstruction. Second, no STM tip-induced migration of physisorbed species was observed during scanning. Third, the partial pressure of gasses within the UHV chamber that are condensable at 77 K is only about

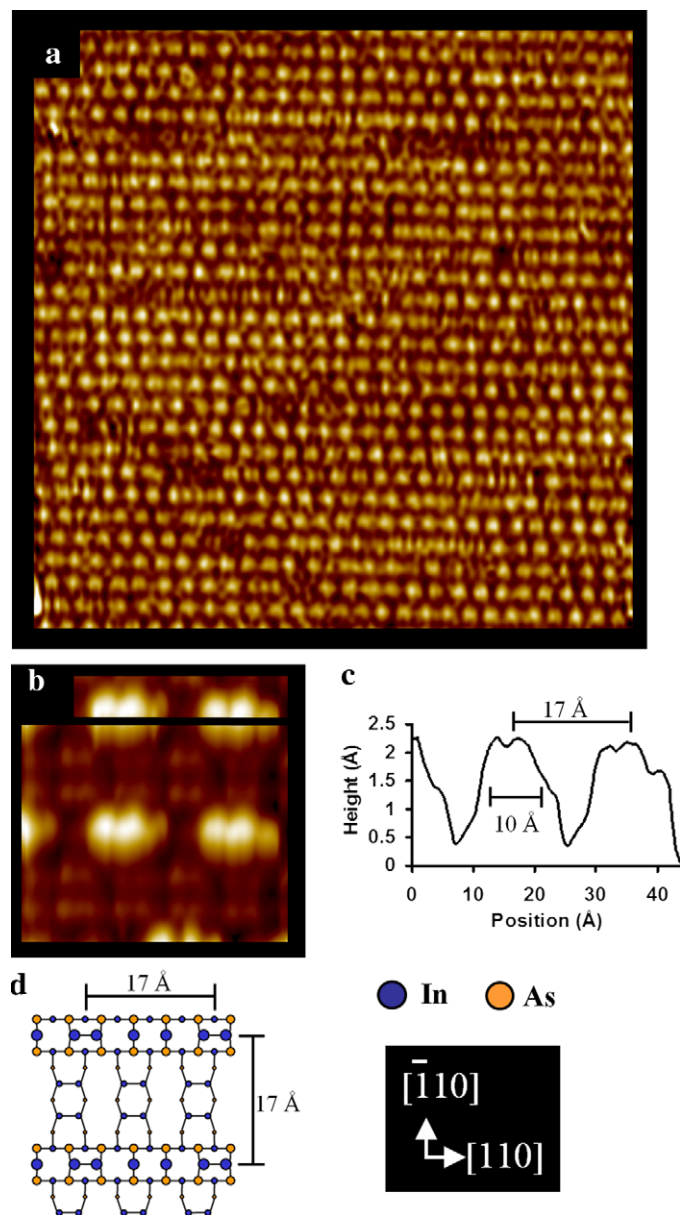


Fig. 4. (a) 450 Å × 450 Å STM image ($V_s = -2.7$ V, $I_t = 0.1$ nA) of the In-Rich InAs(001) surface at 77 K. (b) 33 Å × 33 Å atomically resolved STM image ($V_s = -2.2$ V, $I_t = 0.05$ nA). (c) Line scan corresponding to the black line on the STM image revealing that areas of increased electron density are separated by ~ 17 Å. (d) Ball-and-stick diagram of the $\beta_3'(4 \times 4)$ reconstruction.

1×10^{-12} Torr, and would require several days to reach 1 ML coverage, assuming a sticking probability of unity. Fourth, the change in reconstruction is reversible. In sum, the data supports that the change in reconstruction upon cooling from 300 K to 77 K is solely due to the change in temperature and not condensation of contaminants.

At 77 K, the spacing between areas of high electron density along the rows in the $[1\ 1\ 0]$ direction is ~ 17 Å. Based on the bulk InAs lattice parameter, four In atoms could be accommodated per surface unit cell in the $[1\ 1\ 0]$ along the row. In addition, the transformation from the (4×2) to the (4×4) surface reconstruction is reversible, therefore, both the (4×2) and the (4×4) surface reconstructions must have the same number of surface In atoms. Since the 300 K (4×2) reconstruction has four row In atoms per 17 Å, the In-rich 77 K InAs(001) reconstruction must also have

four row In atoms. Moreover, since the areas of high electron density are ~ 9 Å long (length of areas of high electron density vary from 8 Å to 10 Å depending on the image), two of the In atoms must be dimerized. Since the trough structure visually remains the same for the 300 K and 77 K images it is not necessary to analyze the trough region in the same detail as the row structure.

The height of the row In atoms is dependent on whether the In atoms are dimerized or undimerized. As discussed previously, an undimerized In atom on the row would form one bond each to two second layer As atoms in the $[\bar{1}\ 1\ 0]$ direction (consistent with sp^2 hybridization), which would result in a planar 180° bond angle. Dimerized In atoms, however, would be expected to have a different bonding geometry. In that case the row In atom must bond to two second layer As atoms in addition to an In atom on the row. Since the dimerized In atoms are bonded to three other atoms and have no filled dangling bonds, they would be expected to be sp^2 hybridized. This ideally would result in a planar structure with 120° bond angles. If this ideal structure existed, the height of dimerized and undimerized atoms would be the same. However, simple geometry calculations based on the dimensions of the InAs bulk unit cell reveal for an ideal bonding angle, the In dimer bond distance would be ~ 1.8 Å. The covalent radius of In is 1.63 Å, therefore, the ideal In–In bond length is 3.26 Å [30]. In order to increase the In dimer bond length and reduce overlap in electron density, the In atoms must be forced up out of the plane, causing the bond angles to deviate from 120° . This would cause the dimerized In atoms to image higher in STM images than the undimerized In atoms in the row. Therefore, the most likely low temperature InAs(001) reconstruction is one which has four row In atoms with one pair being dimerized and the other pair of In atoms being undimerized as shown in Fig. 4d. This structure is referred to as the $\beta_3'(4 \times 4)$ reconstruction. Further exploration of this bonding configuration is performed using DFT.

4. Computational results and discussion

4.1. 300 K In-rich InAs(001) reconstruction

The experimental results strongly suggest that the InAs(001)- (4×2) reconstruction observed at 300 K is the $\beta_3'(4 \times 2)$ structure. DFT was used to simulate both the $\beta_3'(4 \times 2)$ (Fig. 5a) and the $\beta_3'(4 \times 2)$ (Fig. 5b) reconstructions. In addition, a highly distorted $\beta_3'(4 \times 2)$ structure (referred to as the $\beta_3'(4 \times 2)$ alternative structure, Fig. 5c, is also identified.

Fig. 5 shows the different fully relaxed reconstructions along with the corresponding energies relative to the $\beta_3'(4 \times 2)$ structure. The lowest-energy structure is the $\beta_3'(4 \times 2)$ alternative structure (Fig. 5c). The $\beta_3'(4 \times 2)$ alternative structure has trough dimers with large distortions, even though the structure is fully relaxed. However, experimentally, trough dimer distortions are not observed at 300 K. It is possible that the trough In dimers are buckled, but flip between buckled positions so rapidly that the trough dimers appear flat in STM images. The flipping dimer phenomenon has been seen on other semiconductor surfaces containing buckled dimers. However, on those surfaces frozen buckled dimers can be seen near defects [31–33]. No frozen trough buckled dimers has ever been observed on the 300 K or 77 K In-rich surfaces.

The discrepancy between the computations and the experiments may result from the periodic boundary conditions required by slab computations. It is possible that the $\beta_3'(4 \times 2)$ alternative structure is the most energetically favored structure if an infinite line of distorted troughs dimers could form. Defects and step edges interrupt the trough dimers, which prevents this from occurring on real surfaces. Therefore, the $\beta_3'(4 \times 2)$ alternative structure will be discarded as a possible structure.

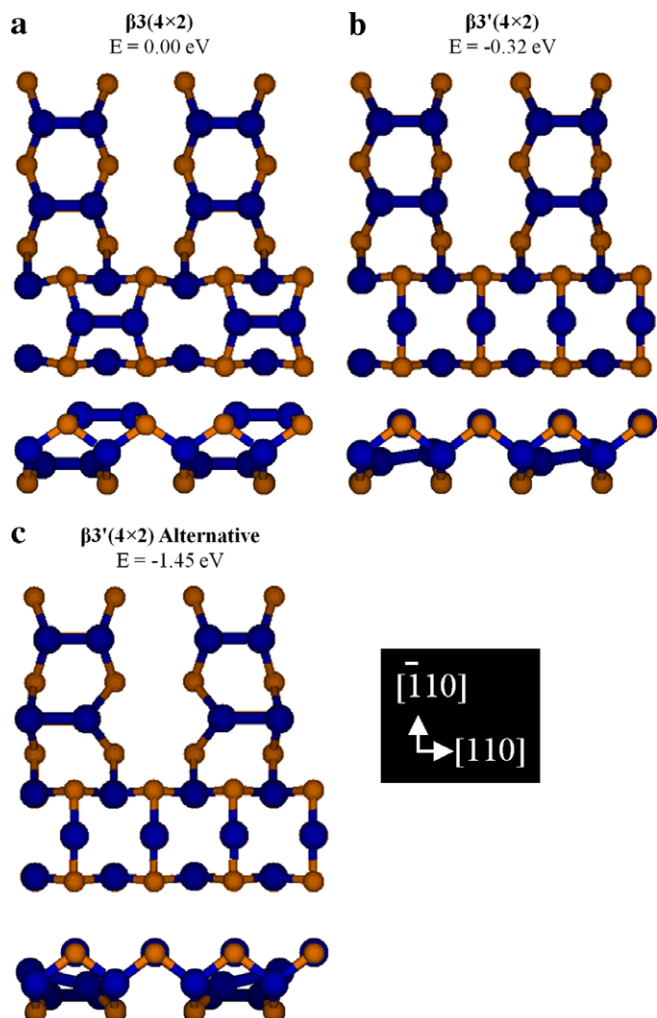


Fig. 5. Top-down (top) and side views (bottom) of the (a) $\beta 3(4 \times 2)$, (b) $\beta 3'(4 \times 2)$, and (c) $\beta 3'(4 \times 2)$ alternative structures computational slabs. Only the top three atomic layers are shown for clarity.

The major difference between the $\beta 3'(4 \times 2)$ structure and the $\beta 3(4 \times 2)$ structure is the bonding environment of the row In atoms. As discussed previously, the row In atoms are dimerized in the $\beta 3(4 \times 2)$ structure; therefore, the row In atoms should be sp^2 hybridized. However the bond angle should be expected to be slightly larger than the ideal 120° for sp^2 hybridized system in order to accommodate the In–In bond. Computationally the As–In–As bond angle is found to be 142° (Fig. 6a) confirming that the out of plane buckling is necessary to relieve strain. Conversely, the row In atoms are undimerized in the $\beta 3'(4 \times 2)$ reconstruction – therefore, they should be sp hybridized. This would result in an As–In–As ideal bond angle of 180° which is in agreement with the bond angle of 179° calculated using DFT (Fig. 6b).

Changes in the hybridization of the surface In atoms should result in changes in the STM images. In the $\beta 3(4 \times 2)$ reconstruction, the row In atoms are positioned higher than the As atoms at the edge of the row (see side-view Fig. 5a). Conversely, the $\beta 3'(4 \times 2)$ structure has In atoms that are sp hybridized, which results in In atoms that are positioned in the same plane as the row edge As atoms and are lower than in the $\beta 3(4 \times 2)$ structure (see side-view Fig. 5b). Moreover, the In dimers have enhanced brightness in STM images since the electron density in the dimer bond is more readily imaged in filled state STM images. The $\beta 3'(4 \times 2)$ structure does not have this electron density originating from the In dimer bonding orbitals resulting in attenuated tunneling from the In row.

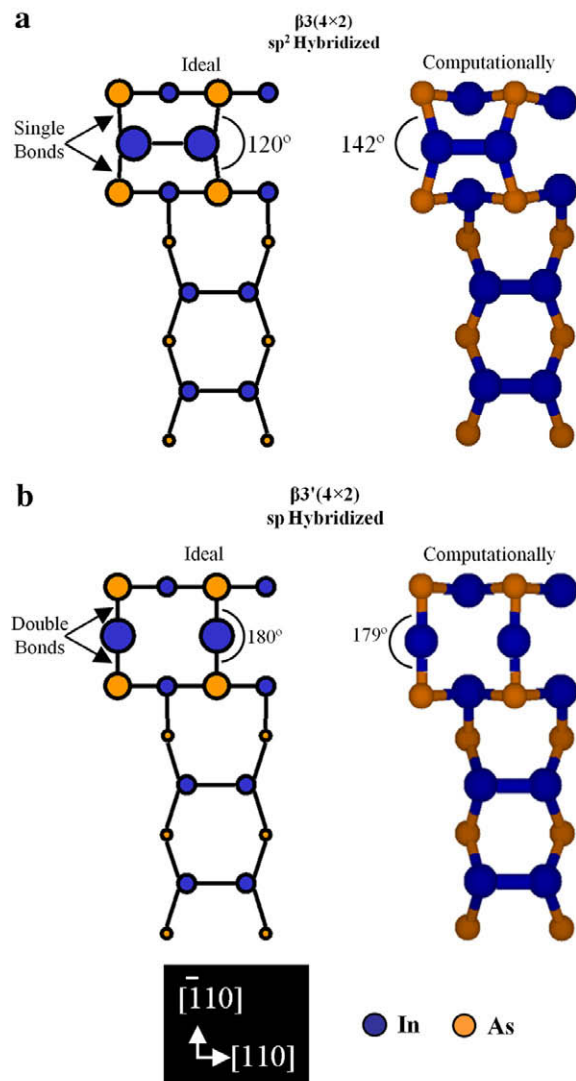


Fig. 6. Ideal and computational bonding angles for the (a) $\beta 3(4 \times 2)$ and (b) $\beta 3'(4 \times 2)$ reconstructions.

Tersoff and Hamann STM simulations were calculated in order to compare the DFT results with the experimental findings [34]. Filled and empty state STM simulations of the $\beta 3(4 \times 2)$ and the $\beta 3'(4 \times 2)$ reconstructions are presented in Fig. 7a and b, respectively. Filled state STM simulations of the $\beta 3(4 \times 2)$ reconstruction have prominent features from the row In dimer. Due to the height difference between the row In atoms and the row edge As atoms, very little electron density from the As atoms is observed. Filled state STM simulations of the $\beta 3'(4 \times 2)$ reconstruction have prominent features from the row edge As atoms because the row In atoms and the row edge As atoms are at the same height. In empty state STM simulations of both the $\beta 3(4 \times 2)$ and $\beta 3'(4 \times 2)$ structures, the majority of the electron density results from the row In atoms. However, the $\beta 3(4 \times 2)$ structure has In dimers and the $\beta 3'(4 \times 2)$ structure has undimerized In atoms. Therefore, the spacing in row-charge-maxima is $\sim 8.5 \text{ \AA}$ for the $\beta 3(4 \times 2)$ structure and $\sim 4.3 \text{ \AA}$ for the $\beta 3'(4 \times 2)$ structure. Experimentally, only charge maxima with $\sim 4.3 \text{ \AA}$ periodicity have been observed at 300 K. Therefore, the $\beta 3'(4 \times 2)$ STM simulation correlates more with the experimental findings at 300 K.

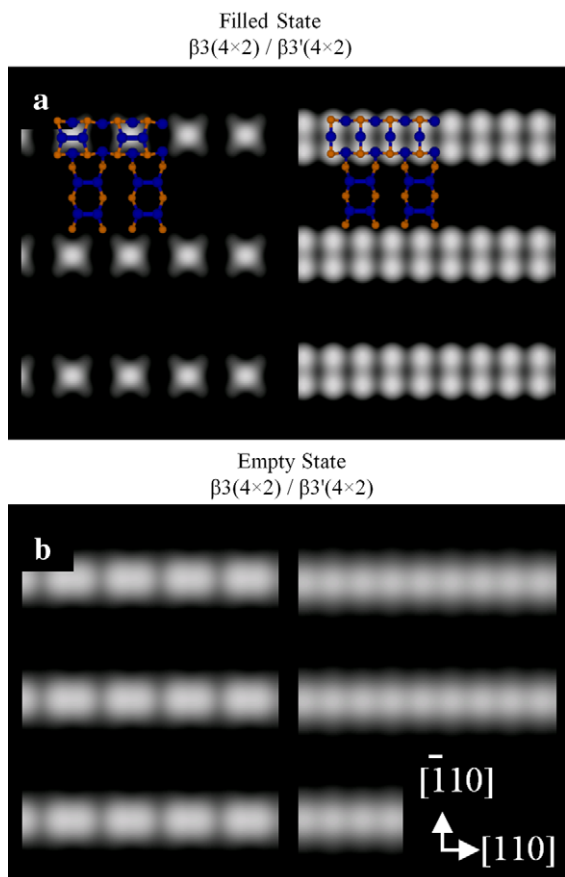


Fig. 7. (a) Filled state STM simulations of the $\beta_3(4 \times 2)$ (top left) and the $\beta_3'(4 \times 2)$ (top right) reconstructions. (b) Empty state STM simulation of the $\beta_3(4 \times 2)$ (bottom left) and the $\beta_3'(4 \times 2)$ (bottom right) reconstructions.

The $\beta_3'(4 \times 2)$ structure is only marginally (-0.16 eV per unit cell) more stable than the $\beta_3(4 \times 2)$ structures, therefore, DFT theory predicts that both structures should be present on the surface at 300 K. However, only the $\beta_3'(4 \times 2)$ reconstruction is observed in STM experiments at 300 K. Several explanations can be given for differences between theory and experiments. First, it is possible that the surface is rapidly converting between the $\beta_3'(4 \times 2)$ and $\beta_3(4 \times 2)$ structures. If the conversion was fast enough, the STM images would be a super-position of the two structures, making the images appear as solely the $\beta_3'(4 \times 2)$ reconstruction. Second, DFT does a poor job of calculating electronic structures of narrow band gap semiconductors such as InAs [35]. The electronic structures of the InAs slabs show a significant overlap between the conduction band and the valence band. This overlap likely causes deviations between the calculated ground state and the actual ground state of the system. Therefore, it is possible that the atomic placements are slightly askew, leading to higher than normal errors in the energy. These errors may be significant enough to alter the energy difference between the two structures.

4.2. 77 K InAs(0 0 1)-(4 × 4) surface

Experimental results strongly suggest that the reconstruction at 77 K is the $\beta_3(4 \times 4)$ reconstruction. Fig. 8 shows top-down and side views of the DFT calculated $\beta_3'(4 \times 2)$ and $\beta_3(4 \times 4)$ structures and their relative energies. The relative energies reveal that the $\beta_3(4 \times 4)$ slab is less stable than the $\beta_3'(4 \times 2)$ slab by 0.04 eV, which is in the error range of DFT and therefore, insignificant.

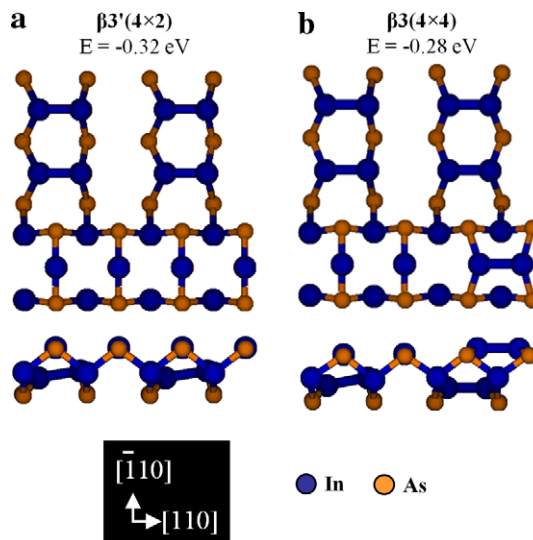


Fig. 8. Top-down (top) and side views (bottom) of the (a) $\beta_3'(4 \times 2)$ and (b) $\beta_3(4 \times 4)$ structures computational slabs. Only the top three atomic layers are shown for clarity.

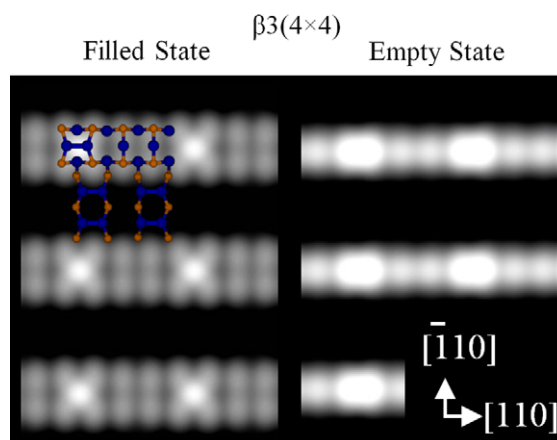


Fig. 9. Filled state (left) and empty state (right) STM simulations of the $\beta_3(4 \times 4)$ reconstruction.

STM simulations of the $\beta_3(4 \times 4)$ reconstruction are shown in Fig. 9. The row structure in both the filled and empty state images is dominated by areas of electron density that are separated by ~ 17 Å. These areas of charge maxima result from the row In dimers. The row In dimers sit higher on the row than the undimerized In atoms and have electron density in their dimer bonds. Therefore, they appear brighter (higher) in STM images. This is consistent with the experimental results.

Although computationally the $\beta_3(4 \times 4)$ structure and the $\beta_3'(4 \times 2)$ structure are energetically degenerate, experimental results acquired at 77 K reveal the existence of only of the $\beta_3(4 \times 4)$ structure, which indicates that it is the most stable structure. The difference between theory and experiment could result from potential errors in calculated ground states associated with narrow bandgap semiconductors as previous discussed.

5. Conclusion

STM images accompanied by DFT calculations identify the 300 K InAs(0 0 1)-(4 × 2) reconstruction as the $\beta_3'(4 \times 2)$ structure. The $\beta_3'(4 \times 2)$ reconstruction has undimerized sp hybridized row In atoms. As the surface is cooled from 300 K down to 77 K, the

reconstruction spontaneously and reversibly changes from the $\beta 3'(4 \times 2)$ reconstruction to the $\beta 3(4 \times 4)$ reconstruction, which has both dimerized, sp^2 hybridized row In atoms, and undimerized, sp hybridized In row atoms. Both the $\beta 3'(4 \times 2)$ reconstruction and $\beta 3(4 \times 4)$ reconstructions have sp hybridized surface atoms which is atypical for III–V surfaces.

Acknowledgements

This work was funded by NSF-DMR-0706243, Intel, SRC-NCRC-1437.003, and the FCRP-MSD-887.011 and Motorola/Freescale Semiconductor, Inc.

Appendix A. Supplementary material

Supplementary data associated with this article can be found, in the online version, at [doi:10.1016/j.susc.2009.09.026](https://doi.org/10.1016/j.susc.2009.09.026).

References

- [1] C. Kittel, Introduction to Solid State Physics, John Wiley & Sons, Inc., Hoboken, 1996.
- [2] M.J. Hale, J.Z. Sexton, D.L. Winn, A.C. Kummel, M. Erbudak, M. Passlack, J. Chem. Phys. 120 (2004) 5745.
- [3] B. Brennan, M. Milojevic, H.C. Kim, P.K. Hurley, J. Kim, G. Hughes, R.M. Wallace, Electrochem. Solid St. 12 (2009) H205.
- [4] C. Kendrick, G. LeLay, A. Kahn, Phys. Rev. B 54 (1996) 17877.
- [5] D.L. Winn, M.J. Hale, T.J. Grassman, J.Z. Sexton, A.C. Kummel, J. Chem. Phys. 127 (2007) 134705.
- [6] H. Xu, Y.Y. Sun, Y.G. Li, Y.P. Feng, A.T.S. Wee, A.C.H. Huan, Phys. Rev. B 70 (2004) 081313.
- [7] J.B. Clemens, S.R. Bishop, D.L. Feldwinn, R. Droopad, A.C. Kummel, Surf. Sci. 603 (2009) 2230.
- [8] Q.K. Xue, Y. Hasegawa, T. Ogino, H. Kiyama, T. Sakurai, Sci. Rep. Res. Tohoku A 44 (1997) 153.
- [9] Q.K. Xue, Y. Hasegawa, T. Ogino, H. Kiyama, T. Sakurai, J. Vac. Sci. Technol. B 15 (1997) 1270.
- [10] Q.K. Xue, T. Hashizume, T. Sakurai, Prog. Surf. Sci. 56 (1997) 1.
- [11] R.H. Miwa, R. Miotto, A.C. Ferraz, Surf. Sci. 542 (2003) 101.
- [12] C. Ratsch, W. Barvosa-Carter, F. Grosse, J.H.G. Owen, J.J. Zinck, Phys. Rev. B 62 (2000) R7719.
- [13] S. Ohkouchi, N. Ikoma, Jpn. J. Appl. Phys. 1 (33) (1994) 3710.
- [14] W.G. Schmidt, Appl. Phys. A-Mater. 75 (2002) 89.
- [15] D.L. Winn, M.J. Hale, T.J. Grassman, A.C. Kummel, R. Droopad, M. Passlack, J. Chem. Phys. 126 (2007) 084703.
- [16] G. Kresse, VASP, Technische University at Wien, 1993.
- [17] G. Kresse, J. Furthmüller, Comput. Mater. Sci. 6 (1996) 15.
- [18] G. Kresse, J. Furthmüller, Phys. Rev. B 54 (1996) 11169.
- [19] G. Kresse, J. Hafner, Phys. Rev. B 47 (1993) 558.
- [20] J.P. Perdew, K. Burke, M. Ernzerhof, Phys. Rev. Lett. 77 (1996) 3865.
- [21] P.E. Blochl, Phys. Rev. B 50 (1994) 17953.
- [22] G. Kresse, D. Joubert, Phys. Rev. B 59 (1999) 1758.
- [23] S.-H. Lee, W. Moritz, M. Scheffler, Phys. Rev. Lett. 85 (2000) 3890.
- [24] J.G. McLean, P. Kruse, J. Guo-Ping, H.E. Ruda, A.C. Kummel, Phys. Rev. Lett. 85 (2000) 1488.
- [25] Refer to the supplementary material published online for this article for an illustrative description of the different energetically degenerate structures of the $a2(4 \times 2)$ reconstruction.
- [26] Y. Liu, A.J. Komrowski, A.C. Kummel, Surf. Sci. 436 (1999) 29.
- [27] M.P. Mikhailova, in: M. Levinshstein, S. Rumyantsev, M. Shur (Eds.), Handbook Series on Semiconductor Parameters, vol. 1, London, 1996, p. 147.
- [28] V.P. LaBella, H. Yang, D.W. Bullock, P.M. Thibado, P. Kratzer, M. Scheffler, Phys. Rev. Lett. 83 (1999) 2989.
- [29] Q.K. Xue, T. Hashizume, T. Sakurai, Appl. Surf. Sci. 141 (1999) 244.
- [30] Handbook of Chemistry and Physics, Boca Raton, CRC Press, 2008.
- [31] R.A. Wolkow, Phys. Rev. Lett. 68 (1992) 2636.
- [32] D. Badt, H. Wengelnik, H. Neddermeyer, J. Vac. Sci. Technol. B 12 (1994) 2015.
- [33] H. Tochihara, T. Sato, T. Sueyoshi, T. Amakusa, M. Iwatsuki, Phys. Rev. B 53 (1996) 7863.
- [34] J. Tersoff, D.R. Hamann, Phys. Rev. B 31 (1985) 805.
- [35] J.P. Perdew, M. Levy, Phys. Rev. Lett. 51 (1983) 1884.